Pertanika J. Sci. & Technol. 32 (5): 2069 - 2081 (2024)

PERTANIKA JOURNALS

SCIENCE & TECHNOLOGY

Journal homepage: http://www.pertanika.upm.edu.my/

The Riblet Short-Slot Coupler Using Substrate Integrated Waveguide (SIW) for High-frequency Applications

Nurehansafwanah Khalid[1], Siti Zuraidah Ibrahim[1,2]*, Mohd Nazri A Karim[1], Wee Fwen Hoon[1,2], Aliya Ashraf Dewani[3], Khuzairi Masrakin[1] and Saidatul Norlyana Azemi[1,2]

[1]Faculty of Electronic Engineering & Technology, Universiti Malaysia Perlis (UniMAP), 02600 Arau, Perlis, Malaysia
[2]Centre of Excellence for Advanced Communication Engineering (ACE), Universiti Malaysia Perlis (UniMAP), 02600 Arau, Perlis, Malaysia
[3]Center for Wireless Monitoring and Applications, School of Electrical Engineering, Griffith University, Brisbane, Australia

ABSTRACT

Substrate Integrated Waveguide (SIW) involves the conductive via holes immersed in a dielectric substrate that connects two substrate plates. This article presents a new SIW technique to enhance the operational bandwidth of the Riblet Short-Slot coupler. To demonstrate the proposed SIW technique, two Riblet Short-Slot couplers are designed and investigated at two different high-frequency ranges, Ku-band and K-band. The bandwidth of the proposed couplers is improved by introducing multiple layers of SIW vias at the center of the couplers' side wall. Applying this approach minimizes the leakage loss between vias, indicating an improved overall operating bandwidth of 36.31% and 26.32% for Ku-band and K-band, respectively. All vias in both prototypes are realized using an alternative method, without using the Plated-Through-Hole Printed-Circuit-Board (PTH-PCB) machine. In addition, experimental results agree well with the simulated results.

ARTICLE INFO

Article history:
Received: 04 September 2023
Accepted: 01 February 2024
Published: 08 August 2024

DOI: https://doi.org/10.47836/pjst.32.5.08

E-mail addresses:
nurehansafwanah@yahoo.com (Nurehansafwanah Khalid)
sitizuraidah@unimap.edu.my (Siti Zuraidah Ibrahim)
nazrikarim@unimap.edu.my (Mohd Nazri A Karim)
fhwee@unimap.edu.my (Wee Fwen Hoon)
a.ashraf@griffith.edu.au (Aliya Ashraf Dewani)
khuzairimasrakin@gmail.com (Khuzairi Masrakin)
snorlyana@unimap.edu.my (Saidatul Norlyana Azemi)
* Corresponding author

Keywords: K-band, Ku-band, Riblet Short-Slot coupler, substrate integrated waveguide

INTRODUCTION

These days, there is a high demand for low loss, high level, and ease of high-frequency integration. Microstrips are essential in producing low-cost and easy fabrication. Recently, some applications have utilized

ISSN: 0128-7680
e-ISSN: 2231-8526

microstrip circuits at low frequencies in the Radio Frequency (RF) range. However, these circuits experience high losses magnetically and electrically (Tu et al., 2022). Therefore, developing and designing RF and microwave integrated circuits with this technology platform is impractical.

Lately, there is considerable interest in planar circuits known as the Substrate Integrated Waveguide (SIW) method as it has many benefits, such as exhibiting low leakage loss (negligible), low insertion loss, and insensitivity to outside interference (Arnieri et al., 2022; Kumar & Raghavan, 2018; Kumar & Rosaline, 2021). The SIW method controls excessive losses through a conducting layer on two sides of a substrate that covers the SIW components. This technology is one of the well-known techniques for transforming the conventional square waveguide into a Printed Circuit Board (PCB) and photo-imageable process (Nayak et al., 2022). This technology is in demand due to its efficiency and high RF and microwave application reliability.

Nonetheless, only a few works of literature are reported on coupler devices that employ the SIW technique for high-frequency applications. For frequency operating lower than 12 GHz, the design of an SIW coupler was successfully established by Sabri et al. (2013), Nasri et al. (2016) and Srivastava et al. (2015). Nevertheless, the presented results in Sabri et al. (2013) and Nasri et al. (2016) are limited to simulation with operational bandwidth of merely 11% in Sabri et al. (2013) and 20% in Nasri et al. (2016). The simulated performance of the SIW coupler in Srivastava et al. (2015) was validated through experiments, but the bandwidth is limited to just 12%. A SIW coupler operating higher than 12 GHz was demonstrated by Carrera et al. (2010). However, the proposed prototypes are not compact due to the usage of numerous vias. A good performance of the SIW coupler with 24% operational bandwidth within a range of 28–38 GHz was verified by Doghri et al. (2015). Nevertheless, it is unpractical to integrate the three-dimensional SIW coupler Doghri et al. (2015) with a planar circuit.

Therefore, a Riblet Short-Slot coupler employing the SIW technique that features a compact size and broader operational bandwidth operating at Ku-band and K-band is demonstrated in this article. The bandwidth of the proposed coupler is enhanced by employing three layers of conductive vias that act as a guiding wall of the coupling section. By employing this approach, the bandwidth is significantly broadened compared to the other SIW coupler designs, which operate at lower operational bandwidth (Carrera et al., 2010; Nasri et al., 2016; Sabri et al., 2013; Srivastava et al., 2015). Furthermore, introducing multiple layers via the coupling sidewall leads to good coupling performance and low insertion loss at the investigated operating frequency range. Two Riblet Shor-Slot couplers are developed and studied at two distinct high-frequency bands, Ku-band and K-band, to demonstrate the proposed SIW approach.

METHODOLOGY

The proposed structure of a Riblet Short-Slot coupler employing a SIW method is illustrated in Figure 1.

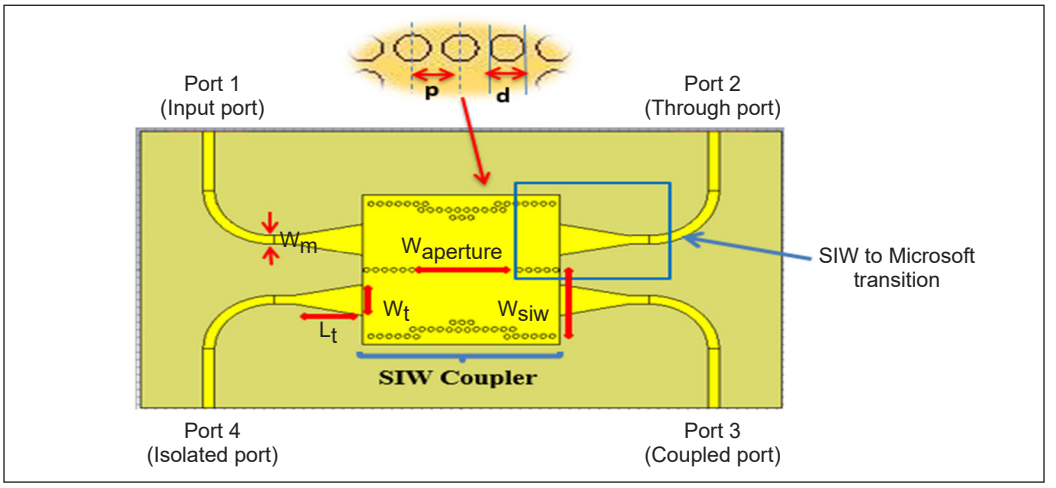

Figure 1. The proposed structure of a Riblet Short-Slot using the SIW technique

The Riblet Short-Slot waveguide coupler is two parallel waveguides with a common sidewall (Haro-Baez et al., 2020; Kumar et al., 2017; Ruiz-Cruz et al., 2011, 2007). The waveguide's sidewall is represented by several vias by means of the SIW technique. The coupler is utilized to distribute the microwave signal through the input port to the two outputs with 90° phase differences between the two output ports. The ports of the coupler in Figure 1 are denoted as an input port (P1), through port (P2), coupled port (P3), and isolated port (P4).

The initial dimensions of the structure in Figure 1 are obtained by determining the width SIW, W_{siw} and W_{equi}, which can be determined through the mathematical Equations 1 and 2 (Aloui et al., 2018; Khalid et al., 2017).

$$W_{siw} = W_{equi} + p(0.766e^{0.4482\frac{d}{p}} - 1.176e^{-1} \quad [1]$$

$$W_{equi} = \frac{c}{2f_c\sqrt{\varepsilon_{eff}}} \quad [2]$$

Where S_{siw} is the width of the Riblet Short-Slot SIW coupler, and W_{equi} is the waveguide port. Moreover, f_c is the cutoff frequency for standard operating frequency, while ε_r is the relative permittivity of the substrate. Note that the following conditions should be fulfilled to reduce leakage loss between vias (Wu et al., 2021):

$$0.5 < \frac{d}{p} < 0.8, \quad [3]$$

where the diameter, *d,* and the pitch of via *p* in Equation 3 are provided as Equations 4 and 5 (Kordiboroujeni & Bornemann, 2014):

$$0.5 < \frac{\lambda_g}{5} \quad [4]$$

$$p \leq 2d \quad [5]$$

$$\lambda_g = \frac{2\pi}{\sqrt{\frac{\varepsilon_r (2\pi f)}{c^2} - (\frac{\pi}{w})^2}} \quad [6]$$

In Equation 6, the cutoff frequency, *c*, is the speed of light, and (ε_r) is the permittivity of the substrate. In the design, d = 0.6 mm is assumed. Therefore, the applicable range for this design is 0.75< p <1.2. The parameter $W_{aperture}$ in Figure 1 is the common sidewall of the Riblet Short-Slot coupler. The length of $W_{aperture}$ is determined using Equation 7 to control the coupling coefficient from input port P1 to the output port P3:

$$W_{aperture} \geq \frac{\lambda_g}{2} \quad [7]$$

To ensure integration compatibility with the planar microstrip technique, the SIW to microstrip taper transition is applied in the design structure in Figure 1. The W_m is the width of microstrip transmission lines that can be determined by Equations 8 to 10 (Kumar et al., 2012):

$$\frac{w}{h} = \begin{cases} \frac{8e^A}{e^{2A}-2} & for\ \frac{w}{h} < 2 \\ \frac{2}{\pi}\left[B - 1 - \ln(2B-1) + \frac{\varepsilon_r - 1}{2\varepsilon_r}\left\{\ln(B-1) + 0.39 - \frac{0.61}{\varepsilon_r}\right\}\right] & for\ \frac{w}{h} > 2 \end{cases} \quad [8]$$

$$A = \frac{Z_0}{60}\sqrt{\frac{\varepsilon_r + 1}{2}} + \frac{\varepsilon_r - 1}{\varepsilon_r + 1}\left(0.23 + \frac{0.11}{\varepsilon_r}\right) \quad [9]$$

$$B = \frac{377\pi}{2Z_0\sqrt{\varepsilon_r}} \quad [10]$$

where Z_0 is the characteristic impedance of the microstrip line. In the design, Z_0 = 50 ohms is assumed. The width of the transition taper, W_t, is determined using Equation 11:

$$W_t = W_m + 0.1547\, W_{siw} \quad [11]$$

where *Wm* is the width of the microstrip transmission lines, and *Wsiw* is the width of the Riblet Short-Slot SIW coupler. The length of the transition taper, *Lt*, can be obtained using Equations 12 and 13.

$$L_t = 0.2368^{\lambda_{g-ms}} \quad [12]$$

$$\lambda_{g-ms} = \frac{\lambda_{g0}}{\sqrt{\varepsilon_{reff}}} \quad [13]$$

Where ($\lambda_{g\text{-}ms}$) is the guided wavelength of the microstrip line, (λ_0) is the wavelength in free space, and (ε_{reff}) is the permittivity, which can be determined using Equation 14 (Aloui et al., 2018).

$$\varepsilon_{reff} = \frac{\varepsilon_r+1}{2}\left(1-\frac{1}{2h}\left(\frac{\varepsilon_r-1}{\varepsilon_r+1}\right)\right)\left(\ln\left(\frac{\pi}{2}\right)+\frac{1}{\varepsilon_r}\ln\left(\frac{4}{\pi}\right)\right) \quad [14]$$

Where h is the thickness of the substrate, the designs are demonstrated at two frequency ranges to validate the proposed Riblet Short-Slot SIW technique (Ku-band and K-band). After optimization of the designs at the center frequency of 14 GHz for Ku-band and 23 GHz for K-band, the final dimensions of the two designs are presented in Table 1.

Table 1
Optimized dimensions of both proposed Riblet Short-Slot SIW coupler

Parameters	Description	Dimension (mm) Ku-band	Dimension (mm) K-band
D	Diameter of via	0.60	0.60
P	Distance between via	0.92	0.92
W_t	Width transition taper	4.13	2.80
L_t	Width of transition taper	7.15	5.26
$W_{aperture}$	Width of aperture	10.92	6.48
W_{siw}	Width of SIW	8.85	6.58
W_m	Width of microstrip TL	1.15	1.10

DESIGN DEVELOPMENT

The SIW Coupler is designed by simulating and analyzing the standard single-row circular metallic via's performance. The parameters, such as the diameter of metallic vias, the pitch between holes waveguide, and the multi-rows of metallic vias with basic rectangular waveguide structures, are studied to initiate the design of the SIW coupler.

The structure of the circular metallic transition on the side wall is designed in layers, as shown in Figure 2. Furthermore, the metallic circular via position is positioned across from another row of via. According to analysis, a broader bandwidth is provided by the triple rows circular metallic via compared to a standard coupler. Additionally, using the suggested SIW coupler, fewer circular metallic via are produced.

As a first step, an SIW is designed with a single row of metallic vias using an equivalent rectangular waveguide model. The E-field distribution is like a traditional rectangular waveguide. The basic waveguide coupler configuration is shown in Figure 2(a). After that, the vias are added in other rows to demonstrate the coupler's performance and effect. As depicted in Figure 2(c), the proposed technique is triple rows of vias, illustrating that vias act as electric side walls to prevent radiation loss.

The magnitude of the electric field of the proposed coupler is shown in Figure 3. The coupling coefficient is optimized such that the sum of the coupled power at port 4 goes to

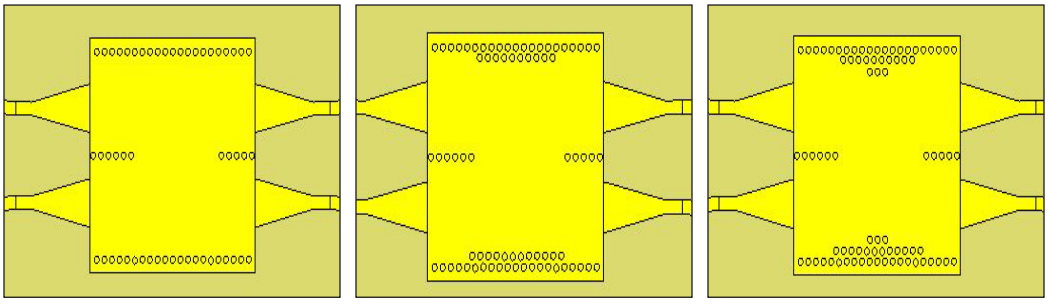

(a) (b) (c)

Figure 2. Evolution structure of SIW coupler: (a) Single rows; (b) Dual rows; and (c) Triple rows

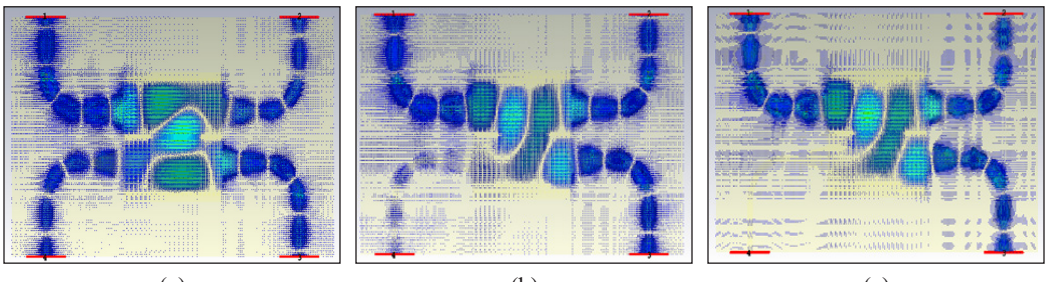

(a) (b) (c)

Figure 3. E-field distribution :(a) Single rows Via; (b) Dual rows Via; and (c) Triple rows Via

zero to exhibit good isolation at that port, as depicted in Figure 3(c). However, the designed coupler with single and dual rows is not in ideal condition, as there is a small amount of signal passing through port 4 (isolated), as illustrated in Figures 3(a) and 3(b).

The parametric analysis is done using an electromagnetic simulation tool to optimize the appropriate number of vias rows. The two rows of side wall vias function as a boundary to avoid leakage and to guide electromagnetic waves.

From Figure 4(a), the single rows via have a narrow operating frequency bandwidth from 12 GHz to 15 GHz. Correspondingly, dual rows via produce a narrow bandwidth that operates from 13 GHz to 17 GHz. We observed better performance with a wide bandwidth of reflection coefficient (S11) in triple rows via, which performed below -40 dB compared to dual rows via, as shown in Figure 4(a). Moreover, Figure 4(b) portrays a better performance of the reflection coefficient (S11), which is triple rows via (at operating frequency 20 GHz to 26 GHz) compared to other layers. Hence, this parametric study validates that the triple rows via perform good SIW coupler performance.

Figures 5(a) and (b) illustrate isolation coefficient (S41) responses for the same variations of rows vias. Based on the results, the parameter of triple rows vias produces the best performance with achieved isolation of more than -45 dB at both operating frequencies. At Ku-band, parameters of dual rows vias and triple rows vias show equal bandwidth

performance. However, the best performance is shown by triple rows vias because the isolation coefficient is more than -50 dB compared to dual rows vias.

As depicted in Figures 6(a) and (b), that graphical result presents the output and transmission coefficient (S21) by different rows of circular metallic via. From Figure 6(a), the basic single rows via is shown slightly above -3 dB in contrast with dual rows via, which are more than -5 dB with amplitude imbalance. Additionally, as shown in Figure 6(b), the triple rows via show a flat amplitude compared to single and dual rows vias. As a result, the dotted lines (green) are producing flat amplitude, and the output transmission coefficient (S21) is shown to be at -3 dB ±1.5 dB. Based on this result, the bandwidth of a coupler with triple rows vias performs higher bandwidth compared to a coupler with single rows vias and dual rows vias.

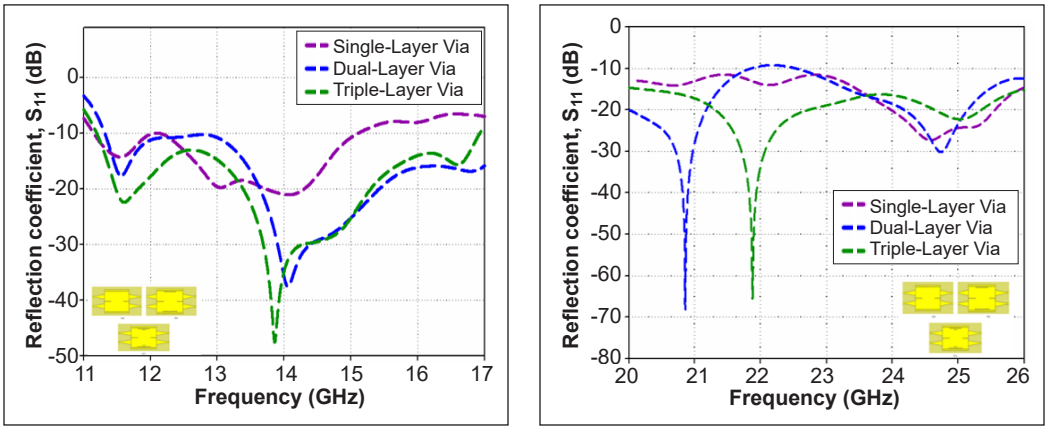

Figure 4. Reflection coefficient, S11 (dB) with different rows of vias: (a) Ku-band; and (b) K-band

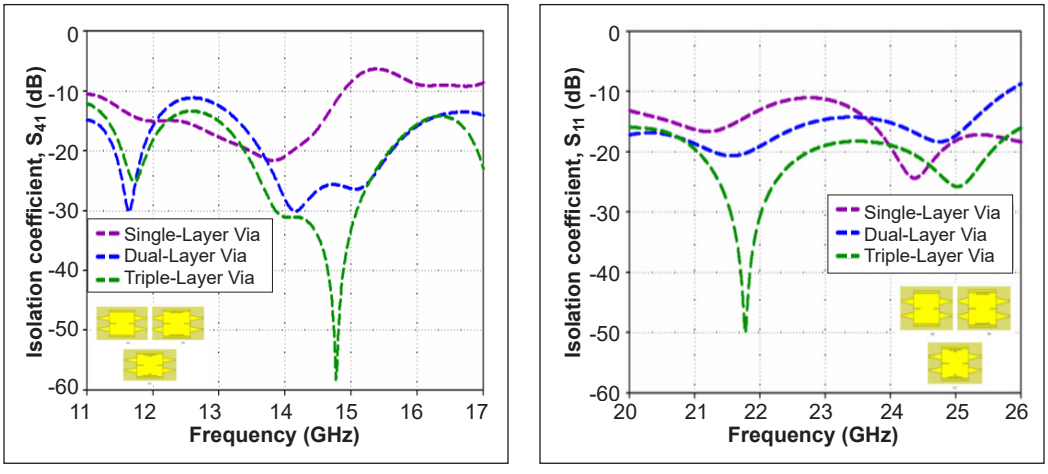

Figure 5. Isolation coefficient, S41 (dB) with different rows of vias: (a) Ku-band; and (b) K-band

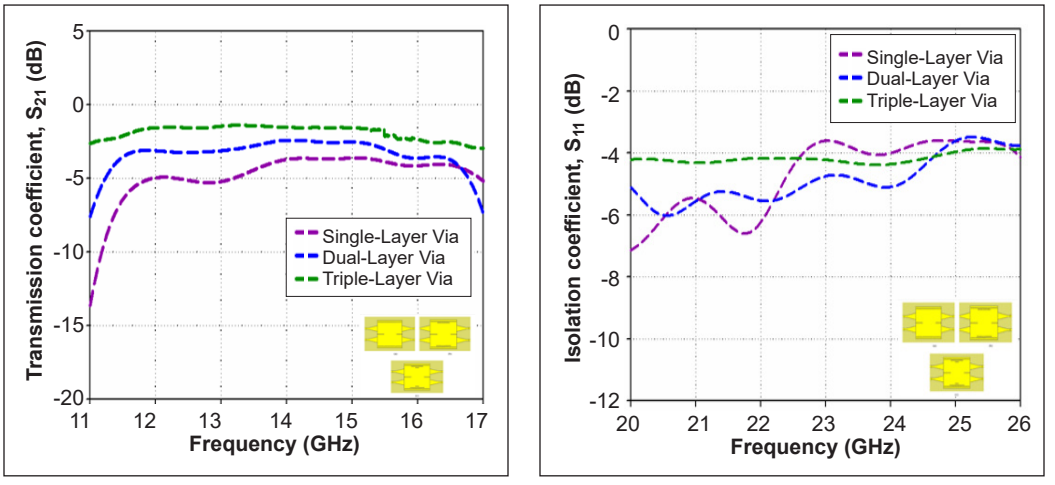

(a) (b)

Figure 6. Transmission coefficient, S21 (dB) with different rows of vias: (a) Ku-band; and (b) K-band

RESULTS AND DISCUSSION

The prototypes for both designs are constructed with the assistance of a Rogers RO4003c substrate with dielectric permittivity ($\varepsilon_r = 3.38$), thickness (h)=0.508 mm, and attenuation (tan θ) = 0.0027. A photograph of both fabricated couplers is displayed in Figure 7. An additional length of tapered microstrip transition is included to attach the SubMiniature version A (SMA) connectors at all ports for measurement purposes. The prototypes of Riblet Short-Slot SIW couplers are fabricated using a PCB machine, and the holes are drilled by a Computerized Numerical Control (CNC) Bungard drilling machine. Finally, the SIW via holes is metalized by soldering all the inserted copper wires into the via holes to ensure the connectivity (ohmic contact) between the conductive layers. By using this approach, it is validated that vias may possibly be constructed using an alternative

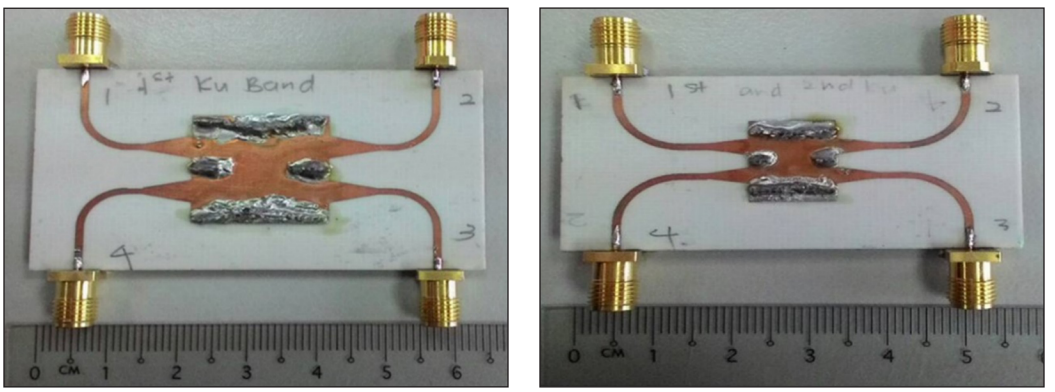

(a) (b)

Figure 7. Photograph of the fabricated prototypes: (a) Ku-band; and (b) K-band

method, as demonstrated in this article, without using the PCB Plated Through Hole (PTH) machine. The final dimensions of the fabricated prototypes are 65 mm × 37 mm and 58 mm × 30 mm for the respective Ku-band and K-band design couplers, including the SIW to microstrip transition length.

The experimental results for the S-parameters performance for both designs are obtained through Agilent PNA-X 5245A PNA Network Analyzer. The simulated and measured S-parameters magnitude for the Ku-band design is illustrated in Figure 8. As displayed in Figure 8, the simulated and measured magnitudes of S11 and S41 are better than 10 dB in the whole operating frequency of Ku-band (12–18GHz). Furthermore, S21 and S31 parameters with coupling coefficients of 3 +-1.5 dB are observed in the same frequency range for both simulated and measured results. Considering all these parameters, a relative bandwidth of 36.31% can be obtained.

There is a slight discrepancy between the proposed SIW coupler's simulated and fabricated performances. A possible reason is dimensional accuracy. The microstrip technique must be fabricated with high precision for high-frequency applications to ensure that it resonates at the desired frequency. Deviations from the desired dimensions can lead to shifts in the resonant frequency or changes in the bandwidth of the resonant response. Errors in the fabrication process, such as non-uniform etching or deposition, can also impact the properties of the SIW and introduce additional scattering or loss.

The simulated and measured results for the K-band coupler are displayed in Figure 9, where the magnitude of S11 and S41 is better than 10 dB in the frequency range of 20–26 GHz. It is observed that the simulated reflection coefficient value of port one, S11, suggests excellent performance with a return loss better than 68 dB at the operating frequency of 21.9 GHz. Furthermore, a 3-dB flat coupling response represented by S21 and S31 parameters is observed in the same frequency range with a tolerance of 0.5 dB. Overall, a bandwidth of 26.32% is obtained for both simulated and measured results based on these parameters.

The phase difference between two output ports is one of the critical parts in the coupler designs, where the simulated and measured Ku-band coupler results are illustrated in Figure 10. Figure 10 indicates a flat phase response with 90° ± 5° is observed within the 11.5 GHz to 16 GHz frequency range. Furthermore, a good response to the simulated and measured phase difference of 90° ± 5° for the K-band design is observed in Figure 11.

The errors between both results are tabulated in Tables 2 and 3 for Ku-band and K-band, respectively, to verify the simulated and measured data. As depicted in Tables 2 and 3, the realized magnitude and phase at the 14 GHz and 23 GHz center frequencies of the simulated and measured S-parameters are very close to the theoretically predicted values. Meanwhile, it can be observed that the computed relative mean error is very low, which makes the proposed design unique and has vastly improved performance. Table 4 presents the comparison between the proposed couplers with previously published works.

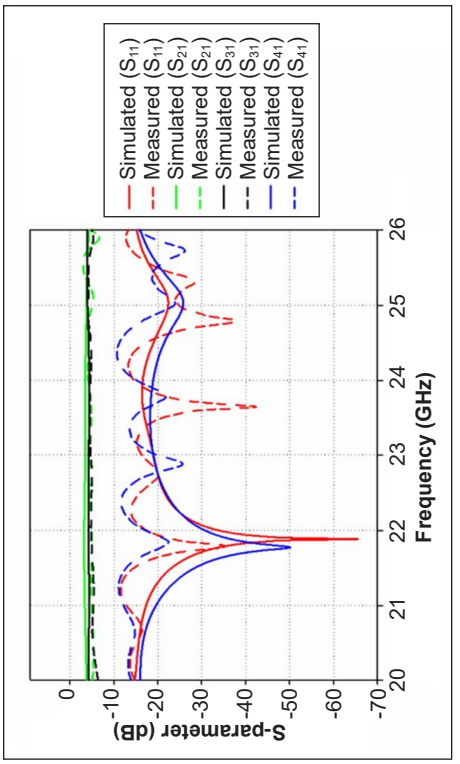

Figure 9. Simulated and measured parameters of K-band

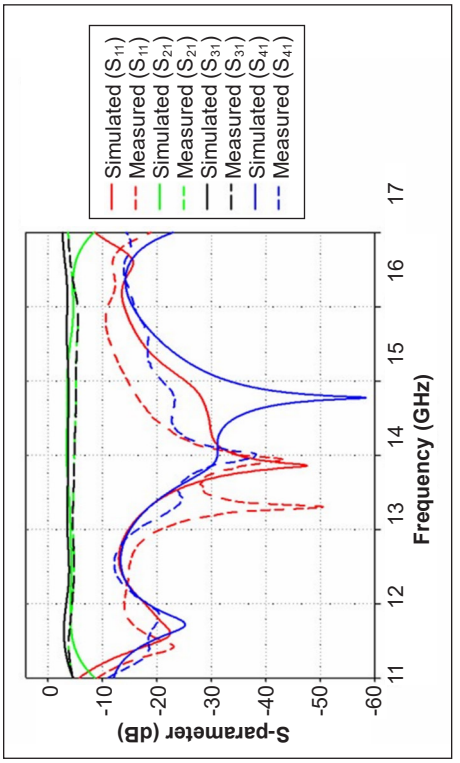

Figure 8. Simulated and measured parameters of Ku-band

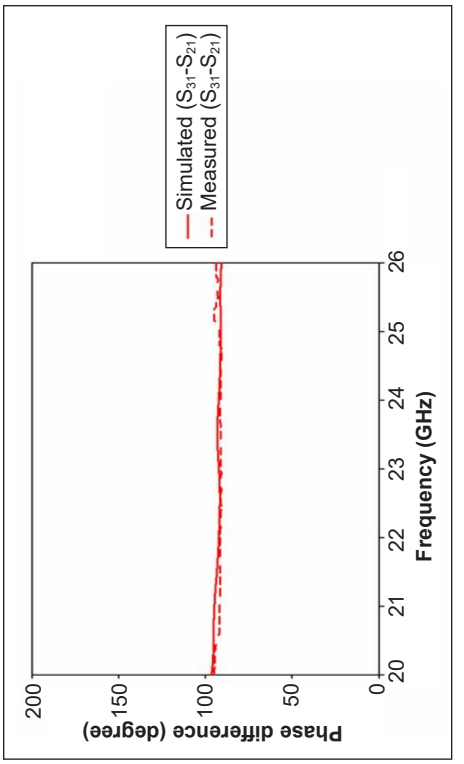

Figure 10. Simulated and measured phase difference of Ku-band coupler

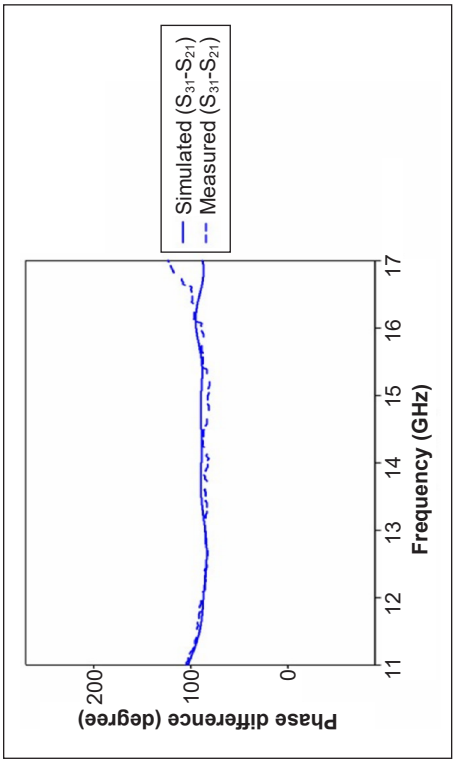

Figure 11. Simulated and measured phase difference of K-band coupler

Table 2
The values simulated against the measured result of the Ku-band coupler

S-Parameters (Ku-band)	S11	S21	S31	S41	S31-S21
Theory (Moscato et al., 2016)	<0.1	0.5/0.355	0.5/0.355	<0.1	90^0±5
Simulation (SM)	0.00	0.47	0.43	0.00	89.67^0
Measurement (M)	0.00	0.33	0.33	0.00	87.00^0
Error btw SM & Theory	-	0.14	0.14	-	0.37
Error btw SM & M	0.00	0.29	0.23	0.00	2.97

Table 3
Simulated against the measured result of the K-band coupler

S-Parameters (K-band)	S11	S21	S31	S41	S31-S21
Theory (Moscato et al., 2016)	<0.1	0.5/0.355	0.5/0.355	<0.1	90^0±5
Simulation (SM)	0.01	0.45	0.44	0.01	92.38^0
Measurement (M)	0.06	0.37	0.38	0.01	91.10^0
Error btw SM & Theory	-	0.10	0.12	-	2.57
Error btw SM & M	0.83	0.18	0.14	0	1.38

Table 4
Performance comparison with other works

S-Parameters (K-band)	S11@S41 (dB)	S21@S31 (dB)	S31-S21	Bandwidth (%)
Sabri et al., 2013	<-10	-3±0.5 dB	90˚±5˚	11
Nasri et al., 2016	<-10	-3±0.5 dB	90˚±5˚	20
Srivastava et al., 2015	<-10	-3±0.5dB	90˚±5˚	12
Doghri et al., 2015	<-10	-3±0.5 dB	90˚±5˚	24
Proposed work	<-10	-3±0.5 dB	90˚±5˚	**Ku-band** (36) **K-band** (26)

CONCLUSION

The proposed Riblet Short-Slot coupler employing SIW technology for Ku-band and K-band frequencies has been successfully simulated and implemented. The designs are performed through multiple layers of sidewall via. A wide bandwidth of 36.31% was obtained in the Ku-band coupler, with return loss and isolation being better than 10 dB and 13 dB, respectively. Moreover, a bandwidth of 26.32% has been accomplished in the K-band coupler with a return loss and isolation higher than 10 dB. Furthermore, the flat phase response of simulated and measured results for both couplers indicates a minimum error. The simulated and measured results mostly agree well over the intended frequency range.

ACKNOWLEDGEMENTS

This research was funded by the Ministry of Higher Education (MOHE), Malaysia, grant number FRGS/1/2019/STG02/UNIMAP/02/5 and the financial support in the form of a publication incentive grant from Universiti Malaysia Perlis (UniMAP), Malaysia. The authors fully acknowledged MOHE and UniMAP for the approved fund, which makes this important research viable and effective.

REFERENCES

Aloui, R., Houaneb, Z., & Zairi, H. (2018, December 16-19). *Modeling a ka-band resonator cavity with SIW 3-D technology*. [Paper presentation]. International Conference on Microelectronics (ICM), Sousse, Tunisa. https://doi.org/10.1109/ICM.2018.8704106

Arnieri, E., Greco, F., Boccia, L., & Amendola, G. (2022). Vertical waveguide-to-microstrip self-diplexing transition for dual-band applications. *IEEE Microwave and Wireless Components Letters, 32*(12), 1407–1410. https://doi.org/10.1109/LMWC.2022.3193166

Carrera, F., Navarro, D., Baquero-Escudero, M., & Rodrigo-Peñarrocha, V. M. (2010, September 28-30). *Compact substrate integrated waveguide directional couplers in ku and k band*s. [Paper presentation]. The 40th European Microwave Conference, Paris, France. https://doi.org/10.23919/EUMC.2010.5616711

Doghri, A., Djerafi, T., Ghiotto, A., & Wu, K. (2015). Substrate integrated waveguide directional couplers for compact three-dimensional integrated circuits. *IEEE Transactions on Microwave Theory and Techniques, 63*(1), 209–219. https://doi.org/10.1109/TMTT.2014.2376560

Haro-Baez, R. V., Ruiz-Cruz, J. A., Córcoles, J., Montejo-Garai, J. R., & Rebollar, J. M. (2020). A new 4 x 4 rectangular waveguide short-slot coupler in 3d printed technology at Ku-band. *Electronics, 9*(4), Article 610. https://doi.org/10.3390/electronics9040610

Juneja, S., Pratap, R., & Sharma, R. (2021). Semiconductor technologies for 5G implementation at millimeter wave frequencies – Design challenges and current state of work. *Engineering Science and Technology, an International Journal, 24*(1), 205–217. https://doi.org/10.1016/j.jestch.2020.06.012

Khalid, N., Ibrahim, S. Z., & Wee, F. H. (2017). Substrate Integrated Waveguide (SIW) coupler on green material substrate for internet of things (IoT) applications. *MATEC Web of Conferences, 140*, Article 01022. https://doi.org/10.1051/matecconf/201714001022

Kordiboroujeni, Z., & Bornemann, J. (2014). New wideband transition from microstrip line to substrate integrated waveguide. *IEEE Transactions on Microwave Theory and Techniques, 62*(12), 2983–2989. https://doi.org/10.1109/TMTT.2014.2365794

Kumar, A., & Raghavan, S. (2018). Planar cavity-backed self-diplexing antenna using two-layered structure. *Progress in Electromagnetics Research Letters, 76*, 91–96. https://doi.org/10.2528/pierl18031605

Kumar, A., & Rosaline, S. I. (2021). Hybrid half-mode SIW cavity-backed diplex antenna for on-body transceiver applications. *Applied Physics A, 127*(11), Article 834. https://doi.org/10.1007/s00339-021-04978-9

Kumar, G. A., Biswas, B., & Poddar, D. R. (2017). A compact broadband riblet-type three-way power divider in rectangular waveguide. *IEEE Microwave and Wireless Components Letters, 27*(2), 141–143. https://doi.org/10.1109/LMWC.2016.2646999

Kumar, H., Jadhav, R., & Ranade, S (2012). A review on substrate integrated waveguide and its microstrip interconnect. *IOSR Journal of Electronics and Communication Engineering, 3*(5), 36–40. https://doi.org/10.9790/2834-0353640

Moscato, S., Moro, R., Pasian, M., Bozzi, M., & Perregrini, L. (2016). Innovative manufacturing approach for paper-based substrate integrated waveguide components and antennas. *IET Microwaves, Antennas and Propagation, 10*(3), 256–263. https://doi.org/10.1049/iet-map.2015.0125

Nasri, A., Zairi, H., & Gharsallah, A. (2016). Design of a novel structure SIW 90° Coupler. *American Journal of Applied Sciences, 13*(3), 276–280. https://doi.org/10.3844/AJASSP.2016.276.280

Nayak, A. K., Filanovsky, I. M., Moez, K., & Patnaik, A. (2022). A broadband coaxial line-to-SIW transition using aperture-coupling method. *IEEE Microwave and Wireless Components Letters, 32*(11), 1271–1274. https://doi.org/10.1109/LMWC.2022.3182933

Ruiz-Cruz, J. A., Montejo-Garai, J. R., & Rebollar, J. M. (2011). Short-slot E- and H-plane waveguide couplers with an arbitrary power division ratio. *International Journal of Electronics, 98*(1), 11–24. https://doi.org/10.1080/00207217.2010.488913

Ruiz-Cruz, J. A., Montejo-Garai, J. R., Rebollar, J. S. M., Daganzo, A. I., & Hidalgo-Carpintero, I. (2007, June 9-15). *Design of riblet-type couplers for Ka band applications*. [Paper presentation]. IEEE Antennas and Propagation Society International Symposium, Honolulu, USA. https://doi.org/10.1109/APS.2007.4396486

Sabri, S. S., Ahmad, B. H., & Othman, A. R. (2013, September 22-25). *Design and fabrication of X-band substrate integrated waveguide directional coupler.* [Paper presentation]. IEEE Symposium on Wireless Technology and Applications (ISWTA), Sarawak, Malaysia. https://doi.org/10.1109/ISWTA.2013.6688784

Srivastava, R., Mukherjee, S., & Biswas, A. (2015, July 19-24). D*esign of broadband planar substrate integrated waveguide (SIW) transvar coupler*. [Paper presentation]. IEEE International Symposium on Antennas and Propagation & USNC/URSI National Radio Science Meeting, Vancouver, Canada. https://doi.org/10.1109/APS.2015.7305090

Tu, H., Hong, H., Zhang, Y., Zhou, L., & Li, X. (2022). The effect of conductive layer thickness on the function of screen printing fabric-based microstrip line. *The Journal of the Textile Institute, 114*(8), 1119-1124. https://doi.org/10.1080/00405000.2022.2109104

Wu, K. E., Bozzi, M., & Fonseca, N. J. G. (2021). Substrate integrated transmission lines: Review and applications. *IEEE Journal of Microwaves, 1*(1), 345–363. https://doi.org/10.1109/JMW.2020.3034379